Journal of Solid Mechanics Vol. 9, No. 1 (2017) pp. 12-23

Bending Analysis of Multi-Layered Graphene Sheets Under Combined Non-Uniform Shear and Normal Tractions

M.M. Alipour [1] , M. Shaban [2,*]

[1]*Department of Mechanical Engineering, University of Mazandaran, Babolsar, Iran*
[2]*Mechanical Engineering Department, Faculty of Engineering, Bu-Ali Sina University, Hamadan, Iran*

Received 2 September 2016; accepted 20 November 2016

ABSTRACT

Bending analysis of multilayer graphene sheets (MLGSs) subjected to non-uniform shear and normal tractions is presented. The constitutive relations are considered to be non-classical based on nonlocal theory of elasticity. Based on the differential transformation method, numerical illustrations are carried out for circular and annular geometries. The effects of nano scale parameter, radius of circular and annular graphene sheet, number of layers as well as distance between layers in the presence of van der Waals interaction forces are investigated. In addition, the effects of different boundary conditions are also examined. The numerical results show that above mentioned parameters have significant effects on the bending behavior of MLGSs under the action of non-uniform shear and normal tractions.

Keywords : Graphene; Multilayer; Nonlocal; Shear and normal traction.

1 INTRODUCTION

GRAPHENE sheets are adjacent nano-plates consisting of monolayer graphite. Due to their honeycomb lattice structure, multi layer graphene sheets has extraordinary and distinctive mechanical and electrical properties that make them valuable in a wide variety of applications in micro and nano-electromechanical systems (MEMS and NEMS) and large amount of research has been dedicated to their applications such as biotechnology, nano-mechanical resonator, etc ([1]-[2]). In the past decade, there are considerable researches focused on the behavior of nano structures by using conventional theories ([3]–[5]). These theories cannot capture intrinsic size-dependence properties of nanostructures. In order to overcome this problem, some scale-based theories such as Cosserat theory, couple stress theory and nonlocal theory are presented. Nonlocal theory is one of the familiar continuum models that includes intrinsic size-dependence in its constitutive equation [6] and great deal of attentions has been devoted to this theory ([7]). This theory has more accuracy compared with experimental results ([8]-[9]). Babaei and Shahidi [10] concerned quadrilateral multi-layered grapheme sheets with simply supported edge conditions. They studied the free vibration behavior of MLGS by using nonlocal theory and showed that number of layer affected the higher modes. Duan and Wang [11] investigated the bending of circular micro and nano-plate. They used variable transformation technique to solve the nonlocal equations. They obtained that considering the nonlocal parameter leads to larger deflections. Lim et al. [12] investigated tortional vibration of nanotubes by considering axial moving of them. They derived their equations by considering history of nonlinear straining with reference to an undeformed state. Murmu and Pradhan [13] studied effect of nonlocal parameter on the free in-plate vibration of nano-plates. In the other work, Pradhan and Phadikar [14] used nonlocal classical and first order plate theory to analyze vibration of

*Corresponding author. Tel.: +98 81 38292505-8; Fax: +98 81 38292631.
E-mail address: m.shaban@basu.ac.ir (M.Shaban).

single and double layer nano-plates. They showed that effect of nonlocal theory becomes more significant when the size of the plate become small. Bi-axial buckling of double-orthotropic nano-plates was investigated by Radić et al. [15]. They focused on the effect of surrounding elastic medium and obtained that considering the elastic medium significantly reduces the impact of small scale effect. Zenkour and Sobhy [16] considered thermal buckling of single layered graphene sheets by using nonlocal sinusoidal shear deformation plate theory. They obtained that results obtained from shear deformation theory are more reliable than those obtained from classical plate theory. Wang and Li [17] studied the bending behavior of single layer rectangular nano-plate by using CPT and FSDT. They presented analytical formulations for simply-supported nano-plates. Narendar and Gopalakrishnan [18] extended nonlocal two-variable refined plate theory to investigate the buckling behavior of orthotropic nano-plate. They showed that buckling load of orthotropic nano-plate is always smaller than that of an isotropic nano-plate.

Farajpour et al. [19] investigated the buckling behavior of circular single-layered graphene sheets (SLGS) under uniform radial compression by using nonlocal elasticity theory. In other work, they considered non-uniformity in the thickness of nano-plate and showed that buckling behavior of SLGS is sensitive to this parameter [20]. Also, Malekzadeh and Farajpour [21] studied axisymmetric vibrations of circular nanoplates under initial in-plane radial stresses by employing Galerkin method. The effects of nonlocal parameter, elastic foundation and initial radial stresses on the natural frequency of the circular nanoplates are investigated by them. Bedroud et al. [22]-[23] presented an analytical solution for buckling analysis of both homogeneous and functionally graded circular/annular Mindlin nanoplates under uniform radial compressive in-plane load.

In other work, Shaban and Alibeigloo[24]–[26] investigated bending and free vibration behavior of single-walled carbon nano-tubes (SWCNTs) based on three-dimensional theory of elasticity. Surveying available literature reveals that up to now no research has been made to study the bending behavior of multilayer graphene sheets (MLGSs) with various boundary conditions and this research attempt to consider this. Furthermore, in the present research, a more general load consists of non-uniform shear and normal tractions are considered. A semi-analytical method based on the differential transform method (DTM) which is successfully used in previous works to determine stresses distribution and natural frequencies of two-directional functionally graded plates ([27]–[29]) is developed in this work to solve the governing equations of MLGSs. In the present study, effects of the van der Wall (vdW) interaction forces between layers are also included in the formulations and influences of these forces are discussed.

2 GOVERNING EQUATIONS

Consider an annular multilayer graphene sheets with outer radius R_o, inner radius R_i and thickness h and *vdW* interaction force field as shown schematically in Fig. 1. For each layer, the Mindlin's plate theory based on the following assumed displacement field

$$u(r,z,t) = u_0(r,t) + z\psi_r(r,t) \qquad w(r,z,t) = w_0(r,t) \tag{1}$$

where u_0, v_0, and w_0 are the radial, circumferential, and transverse displacement components of the mid-surface of the circular plate, respectively. ψ_r is shear rotation of the normal to the middle surface with respect to the radial direction. The strain–displacement equations of linear elasticity are as follow

$$\varepsilon_r = \frac{\partial u}{\partial r} = \frac{\partial u_0}{\partial r} + z\frac{\partial \psi_r}{\partial r},\ \varepsilon_\theta = \frac{u}{r} = \frac{u_0 + z\psi_r}{r},\ \varepsilon_z = \frac{\partial w}{\partial z} = 0,\ \gamma_{rz} = \frac{\partial u}{\partial z} + \frac{\partial w}{\partial r} = \psi_r + \frac{\partial w}{\partial r} \tag{2}$$

In the nonlocal theory, unlike the stress tensor at a reference point in a continuum body depends not only on the strain tensor at that point, but also on the strain tensor of other points. Constitutive model that expresses the nonlocal stress tensor is as follow

$$\left(1 - \mu\nabla^2\right)\sigma_{ij} = t_{ij} = c_{ijkl}\varepsilon_{kl} \tag{3}$$

μ is the nonlocal parameter, σ_{ij} is the nonlocal stress tensor, t_{ij} is the local (classical) stress tensor, c_{ijkl} is the

fourth-order elasticity tensor and ε_{ij} is the local (classical) strain tensor. According to Eq. (2) the constitutive relations for circular and annular nano-plate are given by

$$\begin{aligned}
&\left(1-\mu\nabla^2\right)\sigma_r = \frac{E}{1-\nu^2}(\varepsilon_r + \nu\varepsilon_\theta)\\
&\left(1-\mu\nabla^2\right)\sigma_\theta = \frac{E}{1-\nu^2}(\varepsilon_\theta + \nu\varepsilon_r)\\
&\left(1-\mu\nabla^2\right)\sigma_z = 0\\
&\left(1-\mu\nabla^2\right)\sigma_{rz} = \kappa^2\frac{E}{2(1+\nu)}\gamma_{rz}
\end{aligned} \tag{4}$$

κ^2 denotes the transverse shear correction factor. The stress and moment resultants per unit length defined as below:

$$\begin{Bmatrix} N_{\alpha\beta} \\ M_{\alpha\beta} \end{Bmatrix} = \int_{-h/2}^{h/2} \sigma_{\alpha\beta} \begin{Bmatrix} 1 \\ z \end{Bmatrix} dz, \quad Q_{\alpha\beta} = \int_{-h/2}^{h/2} \tau_{\alpha\beta} dz \tag{5}$$

By substituting Eqs. (2) into Eqs (4) and (5), the following equations can be derived for each layer

$$\begin{aligned}
&\left(1-\mu\nabla^2\right)N_r^{(i)} = A\left(u_{0,r}^{(i)} + \frac{\nu}{r}u_0^{(i)}\right) + B\left(\psi_{r,r}^{(i)} + \frac{\nu}{r}\psi_r^{(i)}\right)\\
&\left(1-\mu\nabla^2\right)N_\theta^{(i)} = A\left(\frac{u_0^{(i)}}{r} + \nu u_{0,r}^{(i)}\right) + B\left(\frac{\psi_r^{(i)}}{r} + \nu\psi_{r,r}^{(i)}\right)\\
&\left(1-\mu\nabla^2\right)M_r^{(i)} = B\left(u_{0,r} + \frac{\nu}{r}u_0^{(i)}\right) + D\left(\psi_{r,r}^{(i)} + \frac{\nu}{r}\psi_r^{(i)}\right)\\
&\left(1-\mu\nabla^2\right)M_\theta^{(i)} = B\left(\frac{u_0^{(i)}}{r} + \nu u_{0,r}^{(i)}\right) + D\left(\frac{\psi_r^{(i)}}{r} + \nu\psi_{r,r}^{(i)}\right)\\
&\left(1-\mu\nabla^2\right)Q_r^{(i)} = \kappa^2\bar{A}\left(\psi_r^{(i)} + w_{,r}^{(i)}\right)
\end{aligned} \tag{6}$$

where

$$\begin{Bmatrix} A \\ B \\ D \end{Bmatrix} = \int_{-h/2}^{h/2} \frac{E}{1-\nu^2} \begin{Bmatrix} 1 \\ z \\ z^2 \end{Bmatrix} dz, \quad \bar{A} = \int_{-h/2}^{h/2} \frac{E}{2(1+\nu)} dz \tag{7}$$

Here, the principle of minimum total energy is used to derive the governing equations.

$$\delta\Pi = \delta U - \delta W = 0 \tag{8}$$

where U and W are the strain energy and work of the externally applied loads, respectively. The variation of strain energy and work of the externally applied loads are as follow,

$$\begin{aligned}
&\delta U = \int\left(\sigma_r^{(i)}\gamma\varepsilon_r^{(i)} + \sigma_\theta^{(i)}\delta\varepsilon_\theta^{(i)} + \tau_{rz}^{(i)}\delta\gamma_{rz}^{(i)}\right)dV,\\
&\delta W = \int\left[q^{(i)}\delta w^{(i)} + T^{(i)}(r)\delta u^{(i)} - C\left(w^{(i)} - w^{(i-1)}\right)\delta\left(w^{(i)} - w^{(i-1)}\right) - C\left(w^{(i)} - w^{(i+1)}\right)\delta\left(w^{(i)} - w^{(i+1)}\right)\right]dA
\end{aligned} \tag{9}$$

where T and P are shear and normal tractions applied to graphene sheets, respectively. i is the layer number and it can be seen that each layer interacted by adjacent top and bottom layer. It is worthy to mention that *vdW* interaction forces between layers are taken into consideration by utilizing springs with constant C. The 1st and n^{th} layers are interacted only by their neighboring layer.

By using Eqs. (1) and (2), Eqs. (9) can be written as follow:

$$\begin{aligned}
\delta U &= \int\left(N_r^{(i)}\delta\frac{\partial u_0^{(i)}}{\partial r} + M_r^{(i)}\delta\frac{\partial \psi_r^{(i)}}{\partial r} + \frac{N_\theta^{(i)}}{r}\delta u_0^{(i)} + \frac{M_\theta^{(i)}}{r}\delta\psi_r^{(i)} + Q_r^{(i)}\delta\left(\psi_r^{(i)} + \frac{\partial w^{(i)}}{\partial r}\right)\right)dA, \\
\delta W &= \int\left[q^{(i)}\delta w^{(i)} + T^{(i)}(r)\delta\left(u_0^{(i)} - \frac{h}{2}\psi_r^{(i)}\right) - C\left(w^{(i)} - w^{(i-1)}\right)\delta\left(w^{(i)} - w^{(i-1)}\right) - C\left(w^{(i)} - w^{(i+1)}\right)\delta\left(w^{(i)} - w^{(i+1)}\right)\right]dA
\end{aligned} \tag{10}$$

By substituting Eq. (10) into Eq. (8), using the theorem of integration by parts and collecting the coefficients of $\delta u_0^{(i)}, \delta\psi_r^{(i)}$ and $\delta w^{(i)}$, three governing equations for i^{th} layer may be derived in the cylindrical coordinate system *(r,θ, z)*

$$\begin{aligned}
&\frac{\partial N_r^{(i)}}{\partial r} + \frac{N_r^{(i)}}{r} - \frac{N_\theta^{(i)}}{r} = -T^{(i)}(r) \\
&\frac{\partial M_r^{(i)}}{\partial r} + \frac{M_r^{(i)}}{r} - \frac{M_\theta^{(i)}}{r} - Q_r^{(i)} = \frac{h}{2}T^{(i)}(r) \\
&\frac{\partial Q_r^{(i)}}{\partial r} + \frac{Q_r^{(i)}}{r} = -q^{(i)} + C\left(w^{(i)} - w^{(i-1)}\right) + C\left(w^{(i)} - w^{(i+1)}\right)
\end{aligned} \tag{11}$$

Considering Eqs. (6), one can obtain the governing Eqs. (11) in terms of displacement components

$$\begin{aligned}
\delta u_0 :&\quad A\left(u_{0,rr}^{(i)} + \frac{u_{0,r}^{(i)}}{r} - \frac{u_0^{(i)}}{r^2}\right) + B\left(\psi_{r,rr}^{(i)} + \frac{\psi_{r,r}^{(i)}}{r} - \frac{\psi_r^{(i)}}{r^2}\right) = -\left(1 - \mu\nabla^2\right)\left(T^{(i)}(r)\right) \\
\delta\psi_r :&\quad B\left(u_{0,rr}^{(i)} + \frac{u_{0,r}^{(i)}}{r} - \frac{u_0^{(i)}}{r^2}\right) + D\left(\psi_{r,rr}^{(i)} + \frac{\psi_{r,r}^{(i)}}{r} - \frac{\psi_r^{(i)}}{r^2}\right) - \kappa^2\bar{A}\left(\psi_r^{(i)} + w_{,r}^{(i)}\right) = \frac{h}{2}\left(1 - \mu\nabla^2\right)\left(T^{(i)}(r)\right) \\
\delta w :&\quad \kappa^2\bar{A}\left(\psi_{r,r}^{(i)} + \frac{\psi_r^{(i)}}{r} + w_{,rr}^{(i)} + \frac{w_{,r}^{(i)}}{r}\right) = \left(1 - \mu\nabla^2\right)\left[-q^{(i)}(r) + C\left(w^{(i)} - w^{(i+1)}\right) + C\left(w^{(i)} - w^{(i-1)}\right)\right]
\end{aligned} \tag{12}$$

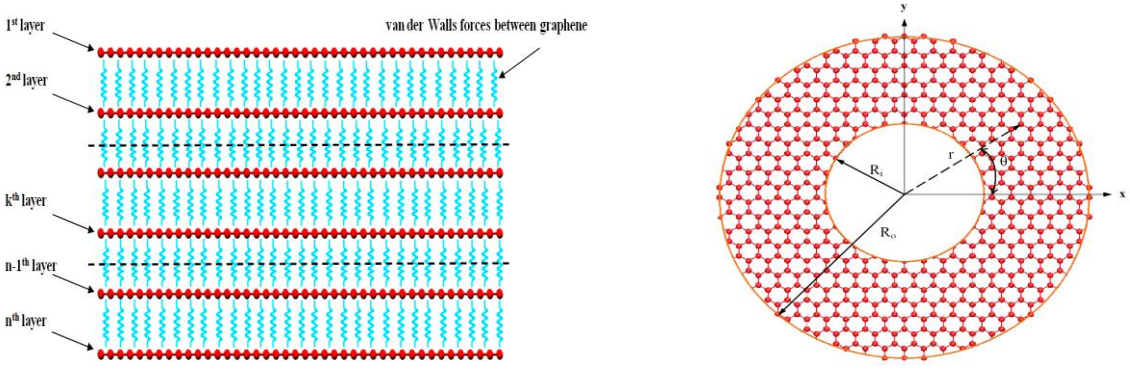

Fig.1
Schematic of Multi layer graphene sheets.

3 SOLUTION PROCEDURE FOR SOLVING GOVERNING EQUATIONS

The set of governing equations are solved by using differential transformation method). The displacement components (u_0 and w_0) and radial rotation ψ_r are analytic in our domain and can be represented by using Taylor power series as follow:

$$u_0^{(i)}(r)=\sum_{k=0}^{\infty}U_k^{(i)}\left(r-r_o\right)^k \qquad w^{(i)}(r)=\sum_{k=0}^{\infty}W_k^{(i)}\left(r-r_o\right)^k \qquad \psi_r^{(i)}(r)=\sum_{k=0}^{\infty}\Psi_k^{(i)}\left(r-r_o\right)^k \tag{13}$$

In the above relations, $U_k^{(i)},W_k^{(i)},\Psi_k^{(i)}$ are the transformed functions in DTM. In this study, non-uniform shear and normal tractions are considered as follow

$$q(r)=\hat{q}\left[\alpha_0+\alpha_1\left(r-r_o\right)+\alpha_2\left(r-r_o\right)^2\right] \qquad T(r)=\hat{T}\left[\beta_0+\beta_1\left(r-r_o\right)+\beta_2\left(r-r_o\right)^2\right] \tag{14}$$

Substituting relations (13) into Eqs. (12), one may obtain three transformed differential equations for governing equations

$$\begin{aligned}&\sum_{k=0}^{N}\Bigg\{A\Bigg[(k+2)(k+1)U_{k+2}^{(i)}-\sum_{l=0}^{k+1}\left(-\frac{1}{r_o}\right)^{l+1}(k-l+1)U_{k-l+1}^{(i)}-\sum_{i=0}^{k}(l+1)\left(-\frac{1}{r_o}\right)^{l+2}U_{k-l}^{(i)}\Bigg]+\\&\quad B\Bigg[(k+2)(k+1)\Psi_{k+2}^{(i)}-\sum_{l=0}^{k+1}\left(-\frac{1}{r_o}\right)^{l+1}(k-l+1)\Psi_{k-l+1}^{(i)}-\sum_{i=0}^{k}(l+1)\left(-\frac{1}{r_o}\right)^{l+2}\Psi_{k-l}^{(i)}\Bigg]\\&-\hat{T}^{(i)}\left[\left(\beta_0-2\mu\beta_2\right)\delta(k)+\beta_1\delta(k-1)+\beta_2\delta(k-2)\right]-\mu\hat{T}^{(i)}\left[\beta_1\left(-\frac{1}{r_o}\right)^{k+1}+2\beta_2\left(-\frac{1}{r_o}\right)^{k}\right]\Bigg\}(r-b)^k=0\end{aligned} \tag{15}$$

Notices that series expansion formulations provided below are used to obtain Eqs. (15)

$$\frac{1}{r}=-\sum_{l=0}^{\infty}\left(-\frac{1}{r_o}\right)^{l+1}(r-r_o)^l \qquad \frac{1}{r^2}=\sum_{l=0}^{\infty}(l+1)\left(-\frac{1}{r_o}\right)^{l+2}(r-r_o)^l \tag{16}$$

To find the solution of Eq. (15), it is required that the coefficient of terms with same powers is set equal to zero and recurrence relations are founded. To obtain the coefficients $\Psi_0^{(i)}$, $\Psi_1^{(i)}$, $U_0^{(i)}$, $U_1^{(i)}$, $W_0^{(i)}$, $W_1^{(i)}$ boundary conditions should be taken into account. Three types for boundary conditions and their transformed forms are given in as follows.

Clamped (C):

$$u_0^{(i)}=\sum_{k=0}^{N+2}U_k^{(i)}(r-r_o)^k=0 \qquad \psi_r^{(i)}=\sum_{k=0}^{N+2}\Psi_k^{(i)}(r-r_o)^k=0 \qquad w^{(i)}=\sum_{k=0}^{N+2}W_k^{(i)}(r-r_o)^k=0 \tag{17}$$

Simply supported (S):

$$u_0^{(i)} = \sum_{k=0}^{N+2} U_k^{(i)} (r - r_o)^k = 0$$
$$M_r = \sum_{k=0}^{N+1} \left[B(k+1) U_{k+1}^{(i)} + \frac{B}{r} U_k^{(i)} + D(k+1) \Psi_{k+1}^{(i)} + \frac{D}{r} \Psi_k^{(i)} \right] (r - r_o)^k = 0 \quad (18)$$
$$w^{(i)} = \sum_{k=0}^{N+2} W_k^{(i)} (r - r_o)^k = 0$$

Free edge (F):

$$N_r^{(i)} = \sum_{k=0}^{N+1} \left[A(k+1) U_{k+1}^{(i)} + \frac{A}{r} U_k^{(i)} + B(k+1) \Psi_{k+1}^{(i)} + \frac{B}{r} \Psi_k^{(i)} \right] (r - r_o)^k = 0$$
$$M_r^{(i)} = \sum_{k=0}^{N+1} \left[B(k+1) U_{k+1}^{(i)} + \frac{B}{r} U_k^{(i)} + D(k+1) \Psi_{k+1}^{(i)} + \frac{D}{r} \Psi_k^{(i)} \right] (r - r_o)^k = 0 \quad (19)$$
$$Q_r^{(i)} = \sum_{k=0}^{N+1} \left[\kappa \bar{A} \Psi_k^{(i)} + \kappa \bar{A} (k+1) W_{k+1}^{(i)} \right] (r - r_o)^k = 0$$

In the center of solid circular graphene sheets, the following conditions should be satisfied:

$$u_0^{(i)} = \sum_{k=0}^{N+2} U_k^{(i)} (-r_o)^k = 0$$
$$\psi_r^{(i)} = \sum_{k=0}^{N+2} \Psi_k^{(i)} (-r_o)^k = 0 \quad (20)$$
$$Q_r^{(i)} = \sum_{k=0}^{N+1} \left[\kappa \bar{A} \Psi_k^{(i)} + \kappa \bar{A} (k+1) W_{k+1}^{(i)} \right] (-r_o)^k = 0$$

4 NUMERICAL RESULTS AND DISCUSSION

First, for comparison purposes, the present analysis was initially restricted and applied to the case of double layer circular graphene sheets subjected uniformly normal traction *q=0.14 MPa* plates having Young's modulus $E=0.396E_c$, $E_c=151$ *Gpa* and Poisson's ratio *v=0.288* and compared with the corresponding results in reference [30]. *C* is *vdW* interaction constant between graphene layers. The non-dimensional deflection is defined as $\bar{w} = \frac{64 D_c}{q r_o^4} w$, $D_c = \frac{E_c h^3}{12(1-v^2)}$. As it is observed from Table 1., there is good agreement between the obtained results and previous researches. Moreover, from Table 1. one can observed that decreasing constant *C*, caused the deflection of upper graphene layer to increased opposite to deflection of lower graphene layer. According to Table 1., one can see that if *vdW* constant, *C*, is significantly large, the springs become rigid and the deflection of two layers be equal. But when this constant become very small, the deflection of first layer has no effect on the deflection of second adjacent layer. In the remaining parts of this study, the material and geometrical properties are assumed as follow: Young modulus *E=2.99 TPa,* thickness *h=0.34 nm, q=100 MPa,* Poisson's ratio *v=0.397*.

Table 2. shows the dimensionless central deflection ($\hat{w}^{(i)} = w^{(i)} / h$) of a simply supported double layer circular graphene sheets under uniformly normal traction for different values of nonlocal parameter, *vdW* interaction constant and outer radius. Similar results presented in Table 3. for double layer fully clamped circular graphene sheets. From these tables, one can observed that irrespective of other parameters, by increasing the nonlocal parameter, μ, the central deflection of first layer, $\hat{w}^{(1)}$ will be decreased. In contrast, the central deflection of second

layer, $\hat{w}^{(2)}$ will be increased. Furthermore, it can be observed that $\hat{w}^{(1)}$ contrary to $\hat{w}^{(2)}$ decreased when the *vdW* constant, *C*, increased. For double layer graphene sheets with larger diameters, however, it is seen from Tables 2. and 3 that both central deflections get almost larger. Also, considering edge condition, the central deflections in clamped circular graphene sheets are always smaller that those with simply supported edge condition.

Table 1
Comparison of dimensionless central deflection, $\bar{w}$ for the double layer circular nano-plate.

B.C	τ		*C*				Ref [30]
			10^{12}	10^{9}	10^{6}	10^{-3}	
Clamp	0.1	$\bar{w}^{(1)}$	1.320	1.565	2.635	2.640	2.639
		$\bar{w}^{(2)}$	1.320	1.075	0.005	5.110×10^{-12}	----
	0.2	$\bar{w}^{(1)}$	1.494	2.442	2.984	2.985	2.979
		$\bar{w}^{(2)}$	1.491	0.543	0.0008	8.321×10^{-13}	----
Simply Support	0.1	$\bar{w}^{(1)}$	5.241	5.507	10.401	10.482	10.481
		$\bar{w}^{(2)}$	5.241	4.976	0.0808	8.207×10^{-11}	----
	0.2	$\bar{w}^{(1)}$	5.415	7.158	10.816	10.827	10.822
		$\bar{w}^{(2)}$	5.412	3.669	0.011	1.010×10^{-11}	----

Table 2
Central dimensionless deflection of simply supported double layer circular nano-plate under uniformly distributed loading.

μ		*r = 1nm*		*r = 2nm*		*r = 5nm*		*r = 10nm*	
(nm²)		$C=5\times10^{18}$	$C=10^{19}$	$C=5\times10^{18}$	$C=10^{19}$	$C=5\times10^{18}$	$C=10^{19}$	$C=5\times10^{18}$	$C=10^{19}$
0	$\bar{w}^{(1)}$	0.001739	0.001706	0.020780	0.018590	0.497578	0.488279	7.66279	7.65541
	$\bar{w}^{(2)}$	3.43×10^{-5}	6.62×10^{-5}	0.004638	0.006827	0.463039	0.472338	7.63326	7.64071
1	$\bar{w}^{(1)}$	0.001583	0.00146	0.017981	0.016005	0.495281	0.487626	7.66276	7.65541
	$\bar{w}^{(2)}$	0.000189	0.000313	0.007437	0.009412	0.465336	0.472991	7.63335	7.64071
2	$\bar{w}^{(1)}$	0.001475	0.001326	0.016615	0.014993	0.493340	0.486773	7.66271	7.65538
	$\bar{w}^{(2)}$	0.000298	0.000447	0.008803	0.010425	0.467277	0.473844	7.63338	7.64076
3	$\bar{w}^{(1)}$	0.001396	0.001243	0.015807	0.014454	0.491792	0.486037	7.66259	7.65529
	$\bar{w}^{(2)}$	0.000377	0.00053	0.009610	0.010963	0.468825	0.47458	7.63359	7.64082
5	$\bar{w}^{(1)}$	0.001288	0.001145	0.014898	0.013894	0.489547	0.484935	7.66197	7.65511
	$\bar{w}^{(2)}$	0.000485	0.000628	0.010520	0.011523	0.47107	0.475682	7.63418	7.64115

Table 3
Central dimensionless deflection of clamped double layer circular nano-plate under uniformly distributed loading.

μ		*r = 1nm*		*r = 2nm*		*r = 5nm*		*r = 10nm*	
(nm²)		$C=5\times10^{18}$	$C=10^{19}$	$C=5\times10^{18}$	$C=10^{19}$	$C=5\times10^{18}$	$C=10^{19}$	$C=5\times10^{18}$	$C=10^{19}$
0	$\bar{w}^{(1)}$	0.000636	0.000632	0.006791	0.006402	0.143469	0.134856	2.00355	1.99615
	$\bar{w}^{(2)}$	4.69E-06	9.26E-06	0.000514	0.000906	0.109737	0.11835	1.97404	1.98143
1	$\bar{w}^{(1)}$	0.00061	0.000585	0.0062	0.005602	0.140572	0.133692	2.00346	1.99613
	$\bar{w}^{(2)}$	3.06E-05	5.59E-05	0.001108	0.001705	0.112634	0.119514	1.97413	1.98146
2	$\bar{w}^{(1)}$	0.000588	0.000551	0.005796	0.005167	0.138571	0.132751	2.00337	1.99611
	$\bar{w}^{(2)}$	5.24E-05	9.03E-05	0.001511	0.00214	0.114635	0.120455	1.97421	1.98148
3	$\bar{w}^{(1)}$	0.00057	0.000524	0.005505	0.004893	0.137092	0.132019	2.00322	1.996
	$\bar{w}^{(2)}$	7.14E-05	0.000117	0.001803	0.002414	0.116114	0.121187	1.97437	1.98158
5	$\bar{w}^{(1)}$	0.000539	0.000487	0.005111	0.004567	0.135038	0.130971	2.00253	1.99568
	$\bar{w}^{(2)}$	0.000102	0.000154	0.002197	0.00274	0.118165	0.122235	1.97505	1.98191

The central dimensionless deflection in *r=2nm* is tabulated in the Table 4. for different number of layers. From Table 4., it is clear that for graphene sheets with higher number of layers, the $\hat{w}^{(i)}$ reduced and distributed among other layers. That is to be expected, because the constraint of clamped boundary condition is stronger than simply supported boundary condition and the $\hat{w}^{(i)}$ is smaller.

Table 4
Central dimensionless deflection of simply supported multi-layer circular nano-plate under uniformly distributed loading (*r=2nm,* S:Simply, C:Clamped).

μ (nm^2)		3 Layer		4 Layer		6 Layer		8 Layer	
		S	C	S	C	S	C	S	C
0	$\bar{w}^{(1)}$	0.018079	0.006389	0.018039	0.006389	0.018034	0.006389	0.018034	0.006388
	$\bar{w}^{(2)}$	0.005401	0.00081	0.005286	0.000808	0.005276	0.000808	0.005276	0.000809
	$\bar{w}^{(3)}$	0.001937	0.000109	0.001542	9.75E-05	0.001507	9.74E-05	0.001507	9.76E-05
	$\bar{w}^{(4)}$	----	----	0.000552	1.3E-05	0.00043	1.17E-05	0.00043	1.17E-05
	$\bar{w}^{(5)}$	----	----	----	----	0.000125	1.4E-06	0.000122	1.4E-06
	$\bar{w}^{(6)}$	----	----	----	----	4.49E-05	1.87E-07	3.5E-05	1.68E-07
	$\bar{w}^{(7)}$	----	----	----	----	----	----	1.02E-05	2.01E-08
	$\bar{w}^{(8)}$	----	----	----	----	----	----	3.64E-06	2.7E-09
1	$\bar{w}^{(1)}$	0.014540	0.005507	0.014272	0.005502	0.014211	0.005501	0.014209	0.005501
	$\bar{w}^{(2)}$	0.006881	0.001385	0.006416	0.001367	0.006312	0.001366	0.006308	0.001366
	$\bar{w}^{(3)}$	0.003996	0.000415	0.002996	0.000339	0.002772	0.000334	0.002764	0.000334
	$\bar{w}^{(4)}$	----	----	0.001733	0.0001	0.001224	8.1E-05	0.001206	8.1E-05
	$\bar{w}^{(5)}$	----	----	----	----	0.000569	1.98E-05	0.000527	1.96E-05
	$\bar{w}^{(6)}$	----	----	----	----	0.000328	5.84E-06	0.000232	4.72E-06
	$\bar{w}^{(7)}$	----	----	----	----	----	----	0.000108	1.15E-06
	$\bar{w}^{(8)}$	----	----	----	----	----	----	6.22E-05	3.39E-07
2	$\bar{w}^{(1)}$	0.012915	0.004969	0.012401	0.004949	0.012232	0.004946	0.012221	0.004946
	$\bar{w}^{(2)}$	0.0074	0.001656	0.006651	0.001607	0.006405	0.001601	0.006388	0.001601
	$\bar{w}^{(3)}$	0.005102	0.000683	0.003774	0.000533	0.003338	0.000517	0.003308	0.000517
	$\bar{w}^{(4)}$	----	----	0.002592	0.000219	0.001765	0.000166	0.001708	0.000166
	$\bar{w}^{(5)}$	----	----	----	----	0.000996	5.47E-05	0.000885	5.3E-05
	$\bar{w}^{(6)}$	----	----	----	----	0.000682	2.23E-05	0.000467	1.7E-05
	$\bar{w}^{(7)}$	----	----	----	----	----	----	0.000263	5.55E-06
	$\bar{w}^{(8)}$	----	----	----	----	----	----	0.00018	2.26E-06
3	$\bar{w}^{(1)}$	0.011975	0.004598	0.011256	0.004557	0.010962	0.004551	0.010932	0.004547
	$\bar{w}^{(2)}$	0.007665	0.001814	0.006704	0.001731	0.006313	0.001717	0.006274	0.001718
	$\bar{w}^{(3)}$	0.005778	0.000896	0.004258	0.000684	0.003637	0.00065	0.003574	0.00065
	$\bar{w}^{(4)}$	----	----	0.003199	0.000336	0.002141	0.000246	0.002034	0.000245
	$\bar{w}^{(5)}$	----	----	----	----	0.001352	9.66E-05	0.001165	9.22E-05
	$\bar{w}^{(6)}$	----	----	----	----	0.001013	4.73E-05	0.000684	3.48E-05
	$\bar{w}^{(7)}$	----	----	----	----	----	----	0.000431	1.36E-05
	$\bar{w}^{(8)}$	----	----	----	----	----	----	0.000323	6.66E-06
5	$\bar{w}^{(1)}$	0.010932	0.004115	0.009912	0.004026	0.009381	0.004005	0.009298	0.004004
	$\bar{w}^{(2)}$	0.007932	0.001991	0.006694	0.001844	0.006045	0.001808	0.005946	0.001807
	$\bar{w}^{(3)}$	0.006554	0.001201	0.00483	0.000897	0.003927	0.000823	0.003788	0.00082
	$\bar{w}^{(4)}$	----	----	0.003981	0.000541	0.002627	0.000379	0.002419	0.000372
	$\bar{w}^{(5)}$	----	----	----	----	0.001886	0.000184	0.001563	0.000169
	$\bar{w}^{(6)}$	----	----	----	----	0.001551	0.00011	0.001043	7.73E-05
	$\bar{w}^{(7)}$	----	----	----	----	----	----	0.000747	3.74E-05
	$\bar{w}^{(8)}$	----	----	----	----	----	----	0.000614	2.24E-05

At the next stage, parametric studies are conducted for annular multi-layers. Table 5. presented the $\hat{w}^{(i)}$ at the r_i*=3.5nm*. In this table, the influences of nonlocal parameter and boundary conditions on the variations of dimensionless deflections are studied. Influence of non-uniformity of shear and normal tractions are studied in Table

6. for circular and annular multi-layer graphene sheets. Also, Table 7. shows the variation of the central deflection of 6 layer annular *GS* for non-uniform tractions and different combinations of boundary conditions. From Table 6., it is observed that the non-uniformity of external loads has a notable effect on the central deflection of circular MLGSs. From Table 7. it is observed that for four different boundary conditions, the annular graphene sheet with clamped-clamped boundary condition has the smallest deflection whereas clamped-free annular graphene sheet has the largest deflection since constraint of boundary conditions become weaker with order of clamped, simply supported and free edge conditions.

Table 5
Dimensionless deflection of multi-layer annular nano-plates at *r=3.5 nm* under uniformly distributed loading ($C=10^{19}$, $r_i=2nm$, $r_o=5nm$).

μ (nm^2)		3 Layer		4 Layer		6 Layer		8 Layer	
		S – S	C - F	S – S	C - F	S - S	C - F	S - S	C - F
0	$\bar{w}^{(1)}$	0.017414	0.025492	0.017346	0.024209	0.017339	0.023702	0.017338	0.023655
	$\bar{w}^{(2)}$	0.005744	0.014716	0.005577	0.012977	0.005559	0.012293	0.005559	0.012228
	$\bar{w}^{(3)}$	0.002334	0.010726	0.001826	0.007916	0.00177	0.006811	0.001769	0.006706
	$\bar{w}^{(4)}$	----	----	0.000742	0.005832	0.000565	0.003915	0.000563	0.003733
	$\bar{w}^{(5)}$	----	----	----	----	0.000185	0.002423	0.000179	0.002099
	$\bar{w}^{(6)}$	----	----	----	----	7.51E-05	0.001789	5.72E-05	0.00121
	$\bar{w}^{(7)}$	----	----	----	----	----	----	1.87E-05	0.000749
	$\bar{w}^{(8)}$	----	----	----	----	----	----	7.6E-06	0.000553
1	$\bar{w}^{(1)}$	0.014517	0.024516	0.014233	0.023072	0.014167	0.02246	0.014163	0.022395
	$\bar{w}^{(2)}$	0.006909	0.015102	0.006426	0.013201	0.006314	0.012397	0.006308	0.01231
	$\bar{w}^{(3)}$	0.004065	0.011316	0.003044	0.008349	0.002806	0.007099	0.002794	0.006964
	$\bar{w}^{(4)}$	----	----	0.001789	0.006312	0.001259	0.004218	0.001231	0.003992
	$\bar{w}^{(5)}$	----	----	----	----	0.000595	0.002706	0.000546	0.002319
	$\bar{w}^{(6)}$	----	----	----	----	0.00035	0.002055	0.000245	0.001385
	$\bar{w}^{(7)}$	----	----	----	----	----	----	0.000116	0.000891
	$\bar{w}^{(8)}$	----	----	----	----	----	----	6.81E-05	0.000677
2	$\bar{w}^{(1)}$	0.013051	0.023728	0.012545	0.02213	0.012378	0.021413	0.012368	0.021329
	$\bar{w}^{(2)}$	0.007382	0.015359	0.006642	0.013302	0.006401	0.01238	0.006384	0.012271
	$\bar{w}^{(3)}$	0.005058	0.011847	0.003743	0.008735	0.003314	0.007343	0.003284	0.007177
	$\bar{w}^{(4)}$	----	----	0.002561	0.006767	0.001746	0.004505	0.001689	0.004236
	$\bar{w}^{(5)}$	----	----	----	----	0.000982	0.00298	0.000873	0.002531
	$\bar{w}^{(6)}$	----	----	----	----	0.000672	0.002314	0.000459	0.001557
	$\bar{w}^{(7)}$	----	----	----	----	----	----	0.000258	0.001031
	$\bar{w}^{(8)}$	----	----	----	----	----	----	0.000177	0.000801
3	$\bar{w}^{(1)}$	0.012161	0.023085	0.011466	0.02134	0.011186	0.020517	0.01116	0.020412
	$\bar{w}^{(2)}$	0.007638	0.015548	0.006704	0.013345	0.006329	0.012306	0.006293	0.012173
	$\bar{w}^{(3)}$	0.005693	0.012301	0.004198	0.009065	0.003598	0.007537	0.00354	0.00734
	$\bar{w}^{(4)}$	----	----	0.003125	0.007185	0.002095	0.004765	0.001994	0.004453
	$\bar{w}^{(5)}$	----	----	----	----	0.001309	0.003242	0.001131	0.002732
	$\bar{w}^{(6)}$	----	----	----	----	0.000974	0.002567	0.000658	0.001725
	$\bar{w}^{(7)}$	----	----	----	----	----	----	0.000411	0.001172
	$\bar{w}^{(8)}$	----	----	----	----	----	----	0.000306	0.000927
5	$\bar{w}^{(1)}$	0.011131	0.022108	0.010153	0.020093	0.009655	0.019059	0.009581	0.018909
	$\bar{w}^{(2)}$	0.007909	0.01581	0.006708	0.013355	0.006096	0.012089	0.006006	0.011903
	$\bar{w}^{(3)}$	0.006452	0.013016	0.004755	0.009592	0.003891	0.00781	0.003763	0.007547
	$\bar{w}^{(4)}$	----	----	0.003875	0.007894	0.002561	0.005206	0.002367	0.004804
	$\bar{w}^{(5)}$	----	----	----	----	0.001813	0.003721	0.001508	0.00309
	$\bar{w}^{(6)}$	----	----	----	----	0.001476	0.003048	0.000992	0.002045
	$\bar{w}^{(7)}$	----	----	----	----	----	----	0.000702	0.001452
	$\bar{w}^{(8)}$	----	----	----	----	----	----	0.000571	0.001184

Table 6
Central dimensionless deflection of 4-layer circular nano-plates under non-uniform shear and normal tractions ($C=10^{19}$, $\hat{T}=\hat{q}=10^8$).

			μ (nm^2)				
			0	1	2	3	5
$\alpha_0=\beta_0=2$ $\alpha_1=\beta_1=1$ $\alpha_2=\beta_2=0$	Clamp	$\bar{w}^{(1)}$	0.009392	0.008093	0.007281	0.006707	0.005926
		$\bar{w}^{(2)}$	0.001233	0.002041	0.002387	0.002565	0.002726
		$\bar{w}^{(3)}$	0.000149	0.000509	0.000797	0.001018	0.001332
		$\bar{w}^{(4)}$	2E-05	0.000151	0.000328	0.000503	0.000805
	Simply support	$\bar{w}^{(1)}$	0.027404	0.021637	0.018777	0.017032	0.014994
		$\bar{w}^{(2)}$	0.008161	0.009864	0.010204	0.010273	0.010239
		$\bar{w}^{(3)}$	0.002385	0.004624	0.005818	0.006559	0.00743
		$\bar{w}^{(4)}$	0.000855	0.002677	0.004002	0.004939	0.006139
$\alpha_0=\beta_0=1$ $\alpha_1=\beta_1=-1$ $\alpha_2=\beta_2=2$	Clamp	$\bar{w}^{(1)}$	0.004696	0.004045	0.00364	0.003353	0.002964
		$\bar{w}^{(2)}$	0.000616	0.001021	0.001194	0.001283	0.001363
		$\bar{w}^{(3)}$	7.47E-05	0.000254	0.000399	0.000509	0.000666
		$\bar{w}^{(4)}$	9.97E-06	7.56E-05	0.000164	0.000251	0.000403
	Simply support	$\bar{w}^{(1)}$	0.013704	0.010816	0.009388	0.008516	0.007497
		$\bar{w}^{(2)}$	0.004079	0.004933	0.005102	0.005136	0.005119
		$\bar{w}^{(3)}$	0.001191	0.002313	0.002909	0.00328	0.003715
		$\bar{w}^{(4)}$	0.000426	0.001339	0.002002	0.002469	0.003069

Table 7
Dimensionless deflection of 6-layer annular nano-plates at $r=3.5$ *nm* under non-uniform shear and normal tractions ($C=10^{19}$, $r_i=2nm$, $r_o=5nm$, $\hat{T}=\hat{q}=10^8$).

$\alpha_0=\beta_0=1$ $\alpha_1=\beta_1=-1$ $\alpha_2=\beta_2=2$		μ (nm^2)				
		0	1	2	3	5
S-C	$\bar{w}^{(1)}$	0.008166	0.007007	0.006286	0.005773	0.005069
	$\bar{w}^{(2)}$	0.001568	0.002143	0.002365	0.002461	0.002513
	$\bar{w}^{(3)}$	0.000299	0.000659	0.000899	0.001063	0.001266
	$\bar{w}^{(4)}$	5.7E-05	0.000204	0.000345	0.000466	0.000653
	$\bar{w}^{(5)}$	1.09E-05	6.46E-05	0.000138	0.000216	0.00036
	$\bar{w}^{(6)}$	2.47E-06	2.54E-05	6.93E-05	0.000124	0.000243
S-S	$\bar{w}^{(1)}$	0.016494	0.013477	0.011776	0.010641	0.009184
	$\bar{w}^{(2)}$	0.005288	0.006007	0.006089	0.006021	0.005799
	$\bar{w}^{(3)}$	0.001683	0.00267	0.003152	0.003423	0.003701
	$\bar{w}^{(4)}$	0.000537	0.001198	0.00166	0.001993	0.002437
	$\bar{w}^{(5)}$	0.000176	0.000566	0.000934	0.001245	0.001724
	$\bar{w}^{(6)}$	7.14E-05	0.000333	0.000639	0.000926	0.001404
C-C	$\bar{w}^{(1)}$	0.005395	0.004353	0.004044	0.003604	0.005395
	$\bar{w}^{(2)}$	0.000713	0.0013	0.001405	0.001503	0.000713
	$\bar{w}^{(3)}$	9.27E-05	0.000392	0.000495	0.000638	9.27E-05
	$\bar{w}^{(4)}$	1.2E-05	0.000119	0.000176	0.000275	1.2E-05
	$\bar{w}^{(5)}$	1.57E-06	3.68E-05	6.47E-05	0.000125	1.57E-06
	$\bar{w}^{(6)}$	2.29E-07	1.41E-05	2.97E-05	7.07E-05	2.29E-07
F-C	$\bar{w}^{(1)}$	0.020636	0.019284	0.018173	0.017261	0.015789
	$\bar{w}^{(2)}$	0.010424	0.010633	0.01068	0.010651	0.010498
	$\bar{w}^{(3)}$	0.005742	0.006067	0.006336	0.00654	0.006825
	$\bar{w}^{(4)}$	0.003296	0.0036	0.003887	0.00414	0.004569
	$\bar{w}^{(5)}$	0.002039	0.002308	0.002571	0.002819	0.003275
	$\bar{w}^{(6)}$	0.001506	0.001753	0.001997	0.002233	0.002688

5 CONCLUSIONS

The bending analysis of MLGSs is studied within the framework of the nonlocal Mindlin's plate theory and by using Hamilton's principle. The external load of MLGS is considered to be non-uniform in both shear and normal directions. It is found that in the MLGSs, unlike SLGSs, nonlocal parameter has a decreasing effect on deflection of first layer whereas this parameter has an increasing effect on other graphene layers. Furthermore, obtained results shows that *vdW* interaction forces have considerable effects in the bending behavior of MLGSs and based on the distance of graphene layers, the equal constant of these forces should be suitably chosen. Several tapes of boundary conditions are examined and effect of them is obtained.

REFERENCES

[1] Chang W. J., Lee H. L., 2014, Mass detection using a double-layer circular graphene-based nanomechanical resonator, *Journal of Applied Physics* **116**(3): 034303.

[2] Gheshlaghi B., Hasheminejad S. M., 2013, Size dependent damping in axisymmetric vibrations of circular nanoplates, *Thin Solid Films* **537**: 212-216.

[3] Gibson R. F., Ayorinde E. O., Wen Y. F., 2007, Vibrations of carbon nanotubes and their composites: A review, *Composites Science and Technology* **67**(1): 1-28.

[4] Behfar K., Naghdabadi R., 2005, Nanoscale vibrational analysis of a multi-layered graphene sheet embedded in an elastic medium, *Composites Science and Technology* **65**(7-8): 1159-1164.

[5] Behfar K., Seifi P., Naghdabadi R., Ghanbari J., 2006, An analytical approach to determination of bending modulus of a multi-layered graphene sheet, *Thin Solid Films* **496**(2): 475-480.

[6] Eringen A. C., 1983, On differential equations of nonlocal elasticity and solutions of screw dislocation and surface waves, *Journal of Applied Physics* **54**(9): 4703.

[7] Rafiee R., Moghadam R. M., 2014, On the modeling of carbon nanotubes : A critical review, *Composites Part B* **56**: 435-449.

[8] Eringen A. C., 2002, *Nonlocal Continuum Field Theories*, Springer.

[9] Lim C. W., 2010, On the truth of nanoscale for nanobeams based on nonlocal elastic stress field theory: equilibrium, governing equation and static deflection, *Applied Mathematics and Mechanics* **31**(1):37-54.

[10] Babaei H., Shahidi A. R., 2011, Vibration of quadrilateral embedded multilayered graphene sheets based on nonlocal continuum models using the Galerkin method, *Acta Mechanica Sinica* **27**: 967-976.

[11] Duan W. H., Wang C. M., 2007, Exact solutions for axisymmetric bending of micro/nanoscale circular plates based on nonlocal plate theory, *Nanotechnology* **18**: 385704.

[12] Lim C. W., Li C., Yu J. L., 2012, Free torsional vibration of nanotubes based on nonlocal stress theory, *Journal of Sound and Vibration* **331**(12): 2798-2808.

[13] Murmu T., Pradhan S. C., 2009, Small-scale effect on the free in-plane vibration of nanoplates by nonlocal continuum model, *Physica E: Low-Dimensional Systems and Nanostructures* **41**(8):1628-1633.

[14] Pradhan S. C., Phadikar J. K., 2009, Nonlocal elasticity theory for vibration of nanoplates, *Journal of Sound and Vibration* **325**: 206-223.

[15] Radić N., Jeremić D., Trifković S., Milutinović M., 2014, Buckling analysis of double-orthotropic nanoplates embedded in Pasternak elastic medium using nonlocal elasticity theory, *Composites Part B* **61:** 162-171.

[16] Zenkour A. M., Sobhy M., 2013, Nonlocal elasticity theory for thermal buckling of nanoplates lying on Winkler–Pasternak elastic substrate medium, *Physica E: Low-Dimensional Systems and Nanostructures* **53**: 251-259.

[17] Wang Y. Z., Li F. M., 2012, Static bending behaviors of nanoplate embedded in elastic matrix with small scale effects, *Mechanics Research Communications* **41**: 44-48

[18] Narendar S., Gopalakrishnan S., 2011, Scale effects on buckling analysis of orthotropic nanoplates based on nonlocal two-variable refined plate theory, *Acta Mechanica* **223**(2):395-413.

[19] Bedroud M., Nazemnezhad R., 2015, Axisymmetric / asymmetric buckling of functionally graded circular / annular Mindlin nanoplates via nonlocal elasticity, *Physica E: Low-Dimensional Systems and Nanostructures* **43**(10):1820-1825.

[20] Farajpour A., Danesh M., Mohammadi M., 2011, Buckling analysis of variable thickness nanoplates using nonlocal continuum mechanics, *Physica E: Low-Dimensional Systems and Nanostructures* **44**(3): 719-727.

[21] Malekzadeh P., Farajpour A., 2012, Axisymmetric free and forced vibrations of initially stressed circular nanoplates embedded in an elastic medium, *Acta Mechanica* **223**(11): 2311-2330.

[22] Bedroud M., Hosseini-Hashemi S., Nazemnezhad R., 2013, Buckling of circular/annular Mindlin nanoplates via nonlocal elasticity, *Acta Mechanica* **224**(11): 2663-2676.

[23] Bedroud M., Nazemnezhad R., 2015, Axisymmetric / asymmetric buckling of functionally graded circular / annular Mindlin nanoplates via nonlocal elasticity, *Meccanica* **50**:1791-1806.

[24] Shaban M., Alibeigloo A., 2014, Static analysis of carbon nano-tubes based on shell model by using three-dimensional theory of elasticity, *Journal of Computational and Theoretical Nanoscience* **11**: 1954-1961.

[25] Shaban M., Alibeigloo A., 2014, Three dimensional vibration and bending analysis of carbon nano- tubes embedded in elastic medium based on theory of elasticity, *Latin American Journal of Solids and Structures* **11**: 2122-2140.

[26] Shaban M., Alipour M. M., 2011, Semi-analytical solution for free vibration of thick functionally graded plates rested on elastic foundation with elastically restrained edge, *Acta Mechanica Sinica* **24**(4): 340-354.

[27] Alipour M. M., Shariyat M., Shaban M., 2010, A semi-snalytical solution for free vibration and modal stress analyses of circular plates resting on two-parameter elastic foundations, *Journal of Solid Mechechanics* **2**(1): 63-78.

[28] Alipour M. M., Shariyat M., 2010, Stress analysis of two-directional FGM moderately thick constrained circular plates with non-uniform load and substrate stiffness distributions, *Journal of Solid Mechechanics* **2**(4): 316-331.

[29] Alipour M. M., Shariyat M., 2011, A power series solution for free vibration of variable thickness mindlin circular plates with two-directional material heterogeneity and elastic foundations, *Journal of Solid Mechechanics* **3**(2): 183-197.

[30] Saidi A. R., Rasouli A., Sahraee S., 2009, Axisymmetric bending and buckling analysis of thick functionally graded circular plates using unconstrained third-order shear deformation plate theory, *Composite Structures* 89(1):110-119.